Applied Composite Materials (2025) 32:1481–1499
https://doi.org/10.1007/s10443-025-10320-w

RESEARCH

Damage Behavior in Unidirectional CFRP Laminates with Ply Discontinuity

M. J. Mohammad Fikry[1,2] · Yutaro Arai[3] · Ryo Inoue[4] · Vladimir Vinogradov[5] · K. T. Tan[2] · Shinji Ogihara[1]

Received: 14 October 2024 / Accepted: 23 February 2025 / Published online: 7 March 2025
© The Author(s) 2025

Abstract
This study presents a comprehensive quantitative investigation into the material properties and damage behavior of unidirectional carbon fiber reinforced plastic laminates with ply discontinuities. Laminates with varying resin gap lengths were evaluated. In situ edge observations and X-ray computed tomography were employed to assess the damage processes in the area of the ply discontinuity. These methods examined initially occurring cracks, secondary cracks, and delamination. Some unexpected cracking behavior was observed in this study. For instance, initial cracks were observed to form not at the interface but at a distance from the resin–ply interface, likely due to a constraint condition caused by the chemical shrinkage of the resin during the curing process. Furthermore, all cracks in the resin region curved toward the center, with successively formed cracks having higher curvatures. This behavior can be attributed to the redistribution of principal stresses within the resin pocket following the initial cracks. The matrix cracking was followed by delamination that started from the tips of the matrix cracks and progressed toward the ends of the specimen. Additionally, the number and locations of cracks in the resin pocket were influenced by the length of the resin gap and the uniformity of the thickness and width of the specimen. In addition to the experimental investigation, a stress-based variational analysis was employed to predict crack onset stresses in the laminates. The analysis successfully calculated the energy release rate for laminates with varying resin pocket lengths and provided predictions for crack onset stresses. The analytical predictions demonstrated good agreement with the experimental observations, enhancing the understanding of resin pocket behavior in CFRP laminates.

Keywords Resin pocket · Fiber discontinuity · Damage behavior · CFRP · Matrix crack · Delamination

1 Introduction

Carbon fiber reinforced plastics (CFRPs), renowned for their high strength-to-weight ratio, are widely used in many industries, including aerospace, automotive, and construction. However, despite their superior mechanical properties, CFRP laminates are prone to damage mechanisms, such as matrix cracks and delamination, that can significantly affect their performance, especially under high loading or fatigue. These damage mechanisms limit the use of CFRPs to structures operating under relatively low strain levels [1–3]. To ensure

Extended author information available on the last page of the article

reliable and cost-effective engineering design, a comprehensive understanding of composite material damage and failure is imperative [4, 5]. Consequently, research efforts have intensified in CFRP damage characterization [6], long-term durability [7], maintenance [8], and health monitoring systems [9]. This increased focus stems from the expanding applications of CFRPs.

Ply discontinuities in composite laminates, whether resulting from tapering [10, 11], material hybridization [6, 12–14], structural modifications [13, 15, 16], or the presence of rivet or bolt holes [17, 18], pose significant challenges in CFRP laminates. Recently, automated fiber placement (AFP) and similar advanced manufacturing technologies have gained significant attention due to their ability to streamline the fabrication of composite structures. However, these technologies often introduce fiber discontinuities and resin pockets, such as those caused by fiber waviness [19, 20]. Such discontinuities are common in cost-effective industrial designs, but they present serious difficulties in maintaining the structural integrity of laminates [21]. These interruptions break the continuity of the fibers, creating weak regions that are highly susceptible to damage. The problem increases in severity in regions with resin pockets or variations in laminate thickness, further increasing stress concentrations and contributing to premature matrix cracking and delamination. Studies have shown that these discontinuities can considerably reduce the durability and reliability of CFRP components, especially under complex loading conditions [22, 23].

Numerous studies have focused on delamination in tapered composite laminates, as it remains a critical damage mode, garnering significant attention in experimental and numerical studies [21, 24]. Fish *et al.* have conducted experimental and analytical investigations on the delamination behavior of tapered composite laminates with multiple internal ply-drop steps [25], revealing that delamination primarily occurs due to interlaminar shear failure of the inter-ply resin surrounding the last ply-drop step. Similarly, Botting *et al.* have explored the delamination strength of glass fiber reinforced plastic (GFRP) laminates with varying ply-drop sequences, showing that the stacking order affects the delamination strength [26]. In line with these findings, Ahamed *et al.* have developed a co-curing ply-overlap joint technique to minimize delamination in hybrid composite structures. Their results showed that strategic design of ply terminations and overlaps can significantly reduce delamination risks, approaching the strength of un-notched glass composites. He *et al.* [27] and Zhang *et al.* [28] have further investigated delamination mechanisms in various laminates, emphasizing the importance of understanding interlaminar stresses in avoiding premature failure.

In addition, Cui *et al.* have conducted an experimental study on unidirectional laminates with cut central plies to focus on delamination, using specimen designs that prevented resin from filling the gap. This approach isolated the delamination behavior, offering clearer insights into the damage processes of the material by eliminating secondary influences. Similarly, this study adopted a simplified specimen design but shifted its focus to investigating the behavior within the resin pocket. In previous studies [23, 29], it has been reported that initial matrix cracks typically form within the resin pocket before delamination cracks propagate into the laminate. This behavior is particularly notable when highly toughened epoxy systems are used. Therefore, understanding the cracking behavior within the resin pocket is crucial for predicting damage progression. Unlike most studies, which have focused on resin pockets in tapered laminates, this research investigates constant-thickness laminates. Using constant-thickness laminates grants a novel perspective on how ply discontinuity and resin accumulation affect damage initiation and propagation without the added complexity of taper-induced stress concentrations. This approach enables a more controlled investigation of resin pocket behavior and its influence on damage mechanisms, as it eliminates the secondary effects caused by thickness variations.

This study intentionally left a gap between the cut plies to be filled with gel-phase epoxy during the curing process, simulating a resin pocket. While other research groups, such as Nakatani et al. [30–32] and Nagata et al. [33], have also utilized similar specimens, experimental observations in this study revealed previously unreported phenomena. Specifically, multiple curved cracks were observed prior to delamination, adding new insight into understanding damage behavior in CFRP laminates. Previous studies [29, 34, 35] presented preliminary findings on this cracking behavior, contributing to the development of variational stress analysis methods for predicting stress distribution and crack formation. However, that earlier work did not provide a systematic quantitative analysis of these observations. Thus, this study fills that gap by offering a comprehensive report on the mechanical properties and damage behavior of unidirectional (UD) CFRP laminates with a ply discontinuity, addressing key gaps in the current literature. In addition to the experimental investigation, this study employs a stress-based variational analysis to predict crack onset stresses in laminates with ply discontinuities. This analysis calculates the energy release rate (ERR) for laminates with varying resin pocket lengths and provides predictions for the location and critical stresses associated with crack initiation. By integrating experimental findings with analytical predictions, this research not only enhances the understanding of resin pocket behavior but also demonstrates the potential of variational analysis as a complementary tool for predicting damage progression in CFRP laminates with complex internal structures (Fig. 1).

2 Material and Methods

2.1 Specimen Manufacturing

A series of UD $[0]_8$ laminates with discontinuous plies was fabricated using an autoclave. The material used was CFRP prepreg composite, specifically T700SC/2592 (Torayca), with a ply thickness of 0.14 mm. During the elevated temperature curing process, the gel-phase epoxy resin in the surrounding CFRP plies filled the gap between the plies, forming a resin pocket, which was subsequently cured with the rest of the laminate. The laminates consisted of four discontinuous plies in the middle, with varying lengths of resin gaps. To create the laminates, a stack of four plies of the prepreg was cut in half perpendicular to the fiber direction. The cut plies were then aligned with a defined gap ranging from 0.03 to 3 mm. The specimens and their corresponding post-cured gap lengths are listed in Table 1. Subsequently, two continuous $[0]_2$ UD laminates were placed on the top and bottom of the stack, forming a symmetrical laminate configuration as shown in Fig. 2. The stacked prepregs were then

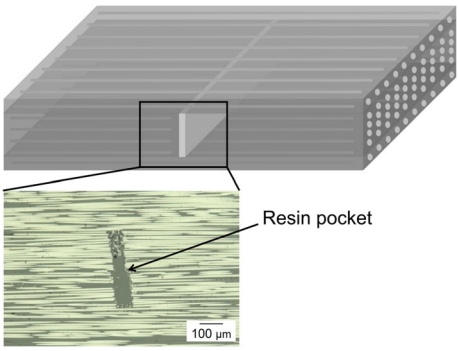


Fig. 1 A CFRP laminate with a resin pocket

Table 1 Post-cured resin gap length of each representative specimen

Specimens	post-cured resin gap length
1	30.9 μm
2	1.38 mm
3	1.73 mm
4	3.41 mm

placed between aluminum plates with Teflon (PTFE) sheets, vacuum-sealed using bagging film and double-sided tape, and covered with a breather. The laminate was then cured in an autoclave under vacuum, following a two-stage cycle: 90°C at 0 MPa for 60 min, then 130°C at 0.2 MPa for 270 min. The resulting averaged post-cured thickness of the laminate was approximately 1.18 mm. Finally, the laminates were cut into specimens of the dimensions shown in Fig. 2 using a composite material cutting machine. To facilitate testing, 50-mm-long glass fiber/epoxy end tabs were securely bonded to both ends of the specimens.

2.2 Tensile Testing and Damage Observation

A strain gauge setup was implemented to measure the strain. One strain gauge, referred to as strain gauge 1, was affixed directly above the resin pocket within the ply discontinuity region, as illustrated in Fig. 2. Another strain gauge (strain gauge 2) was positioned 20 mm from the center of the ply discontinuity region. The strain gauges used in the study were 5-mm uniaxial strain gauges (KFGS-5-120-C1-11L1M2R, Kyowa). Strain gauge 1, located on top of the ply discontinuity region, was used to measure the strain in the laminate affected by the presence of the resin pocket. This strain measurement provides insights into the mechanical properties of the laminate influenced by the resin pocket. In contrast, strain gauge 2 was positioned 20 mm from the center of the ply discontinuity region. This placement captured the linear properties of the stress and strain in the part of the laminate without ply discontinuities. The strain measured by strain gauge 2 represents the strain behavior in a laminate without any ply discontinuities.

Two types of tensile loading were performed on the specimens: monotonic loading and loading–unloading. The tensile tests were conducted using a TENSILON RTF-1350 (A&D) tensile testing machine, similar to the one used in [36–38]. The crosshead speed

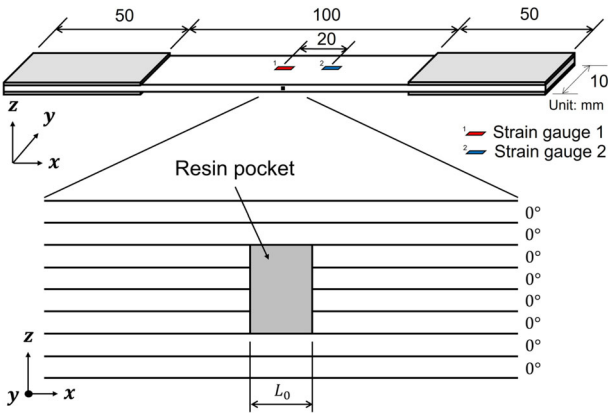


Fig. 2 Specimen measurements, lamination structure, and strain gauge placements

during the tests was set to 0.5 mm/min. This crosshead speed was selected to enable in situ edge observation of the damage behavior. Two types of microscopes were used: an in situ optical microscope, VHX-1000 (KEYENCE), and a static optical microscope, VHX-2000 (KEYENCE). Before observations, the specimen edges were polished using a polishing machine, TegraPol-15 (Struers Inc.). The polishing procedure used water-resistant abrasive papers: #1000 for three minutes, followed by #2000 and #4000 for eight minutes each. Subsequently, a polishing cloth with diamond spray (DP-spray, Struers) was applied to the edges for an additional three minutes.

To visualize the initiation and progression of damage within the opaque CFRP laminates, three-dimensional observations were made using X-ray computed tomography (CT) using a multiscale X-ray computed scanner (SkyScan2214, Bruker). Transmitted images of the sample were taken every 0.2° while the sample was rotated, and a total of 1801 images were obtained using a CCD sensor with a resolution of 4032 x 2688 pixels (3 x 3 μm/pixel). The source voltage, current, and target power were 30 kV, 130 μA, and 0.69 W, respectively.

3 Results and Discussion

3.1 Mechanical Properties

The mechanical properties of the UD laminate with various resin gap lengths, as obtained from the monotonic tensile tests, are presented in Table 2. In Fig. 3, the corresponding stress–strain curves for laminates with resin gap lengths of 30.9 μm, 1.38 mm, 1.73 mm, and 3.41 mm are shown. Only representative specimens for each resin gap length are shown in Fig. 3.

As observed in Table 2, the stress–strain curve gradient measured by strain gauge 1 was consistently lower than that measured by strain gauge 2 for all laminates. This indicates that the presence of a ply discontinuity significantly degraded the local stiffness of the laminates. The gradient of the stress–strain curve (at strain gauge 1) decreased as the resin gap width increased. For the laminate with a very short resin gap of 30.9 μm, the decrease in the gradient (measured by strain gauge 1) was much smaller, only 2% (see Fig. 3(a)). In contrast, for resin gap lengths of 1.38, 1.73, and 3.41 mm, the decreases were 28%, 43%, and 39%, respectively. The decrease in stiffness with increasing resin gap width can be attributed to the stress distribution and load transfer mechanisms in the laminate. Since the resin has a much lower modulus than the fibers, this reduces the local stiffness, leading to a lower gradient in the stress-strain curve. Before a crack occurred (indicated by non-linearity in the stress–strain curve), the curves of strain gauges 1 and 2 overlapped. However, although the other specimens exhibited cracks at lower stresses, the slopes of the stress–strain curve at strain gauge 1 were lower than the one at strain gauge 2, even at much lower stress levels (as shown in Fig. 3(b)–(d)). This indicates that until certain stress or strain levels just prior to the damage, the presence of a very short resin pocket (ply discontinuity) did not significantly affect the stiffness of the laminate.

The measurements from strain gauge 2 of all specimens (Fig. 3 (a)–(d)) confirmed linear elastic stress–strain behavior between crack occurrences until the occurrence of delamination. The slope from strain gauge 1 of the specimen with a very short resin gap gradually decreased after the first non-linearity (occurrence of a crack), demonstrating a gradual increase of the delamination area between continuous and discontinuous plies compared to other specimens (see Fig. 3 (a)). Also, the readings from strain gauge 1 in the specimens with longer resin gaps showed multiple strain jumps as multiple cracks occurred in the resin pocket. However,

Table 2 Mechanical properties from monotonic tensile test

Specimen	Properties	Strain 1	Strain 2	Fracture stress [MPa]
1	Gradient, [GPa]	117	119	1112
	Fracture strain [%]	1.94	1.81	
2	Gradient, [GPa]	92.6	124	1209
	Fracture strain [%]	1.68	1.77	
3	Gradient, [GPa]	79.4	140	1381
	Fracture strain [%]	2.01	1.89	
4	Gradient, [GPa]	78.2	129	1289
	Fracture strain [%]	1.94	1.96	

these slopes are more linear than the specimen with a shorter resin gap, which showed a slower progression of delamination (e.g., strain gauge 1 in Fig. 3 (d)).

Furthermore, in Fig. 3 (a), there is an significant strain increase at a constant stress of 660 MPa, which occurs due to the complete separation by delamination between continuous and discontinuous plies. After this, both strain gauges measured only the strain of the outer (continuous) plies, as only they now held the loads. This corresponds to the complete discount of the four (discontinuos) middle plies contribution to the local laminate stiffness.

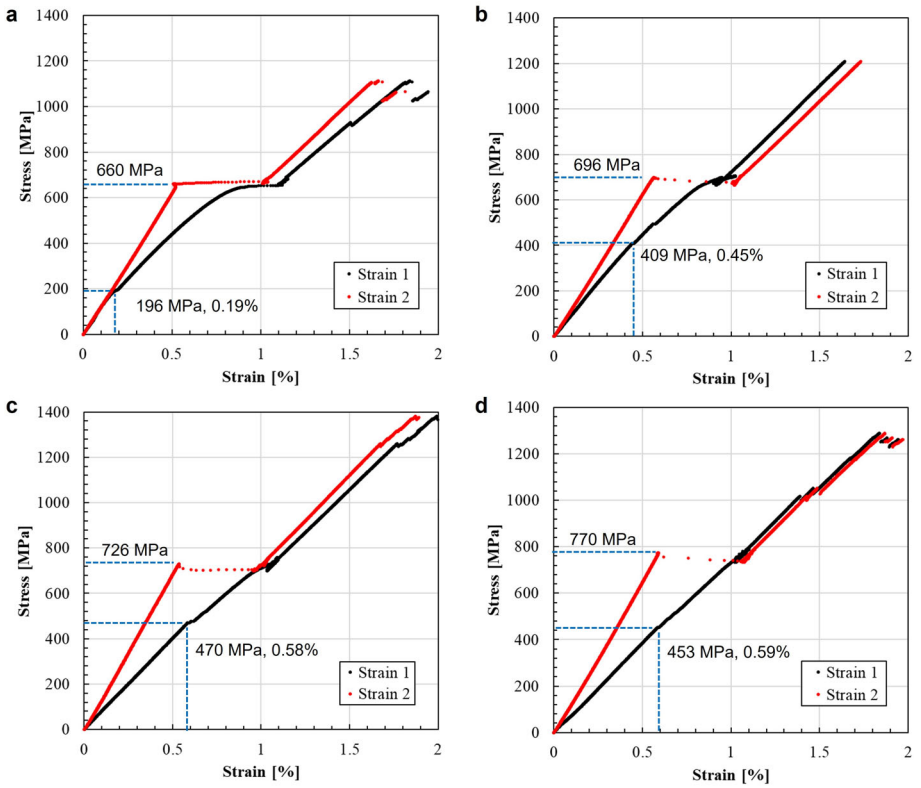


Fig. 3 Stress–strain curve from the monotonic tensile test of UD laminate with resin gap lengths of (a) 30.9 µm (Specimen 1), (b) 1.38 mm (Specimen 2), (c) 1.73 mm (Specimen 3), and (d) 3.41 mm (Specimen 4)

This behavior was observed in all specimens. Comparing the results, complete separations occurred faster in specimens with a small resin gap compared to specimens with a longer resin gap: at 660 MPa for a 30.9-µm resin gap, at 681 MPa for a 1.38-mm resin gap, at 726 MPa for a 1.73-mm resin gap, and 770 MPa for a 3.41-mm resin gap. The initiation timing of the crack and delamination in each specimen might influence this. The optical observations of the edges at this stage are discussed in the next section to validate these results.

3.2 Damage Observation

Figure 4 shows the optical observations of crack appearance with an increasing tensile load at the edge of the specimens and the corresponding average applied stress in the laminate specimen with the resin gap length of 30.9 µm (Specimen 1). Specimen 1 represents the results for a laminate with a very short resin gap (<0.1 mm), as similar damage behavior was observed in all other specimens. A total of four specimens with similar resin pocket lengths were tested. As seen in Fig. 4, a single crack appeared at the edge of the specimen in the resin pocket at an applied stress of 196 MPa, which resembled the first strain jump phenomena in the stress–strain curve in Fig. 3 (a). Matrix cracking was followed by delamination cracks that gradually grew in the opposite directions from the matrix cracks toward the ends of the specimen (see Fig. 4 at applied stresses of 433 and 653 MPa). This observation also reflected a decrease in the stress–strain curve slope as seen in Fig. 3 (a) after 433 MPa, indicating delamination. However, it is unclear whether the crack here was located precisely at the interface between the resin and the discontinuous UD ply or in the middle of the resin, as the resin gap is too short and its geometry (fiber cut lining) is uneven. However, it was assumed that the crack occurred at the interfaces because, at the edge corner of the resin pocket, it followed the shape of the interfaces (see Fig. 4 at applied stress of 433 MPa).

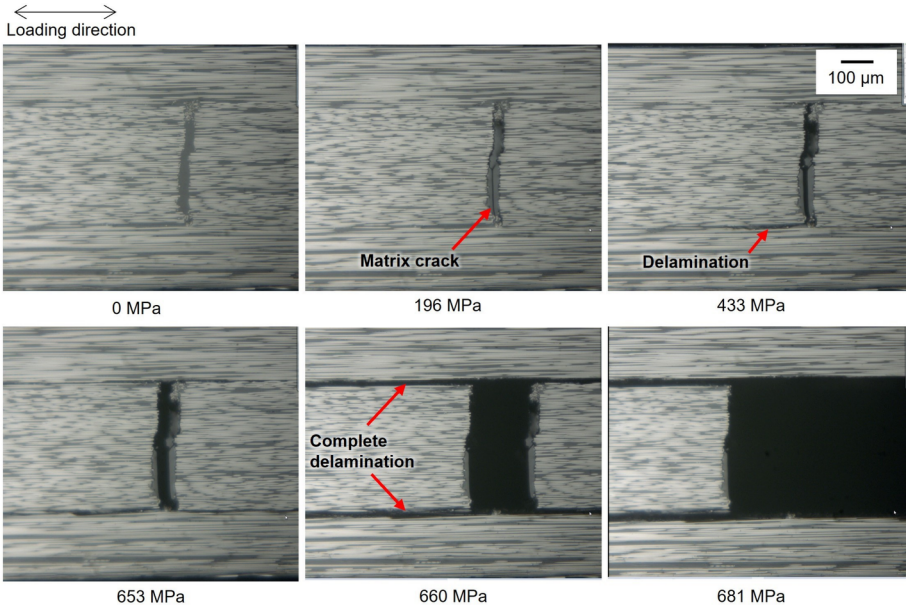


Fig. 4 Microscopic images of laminate edge (specimen 1) with 30.9-µm resin gap at different stress levels

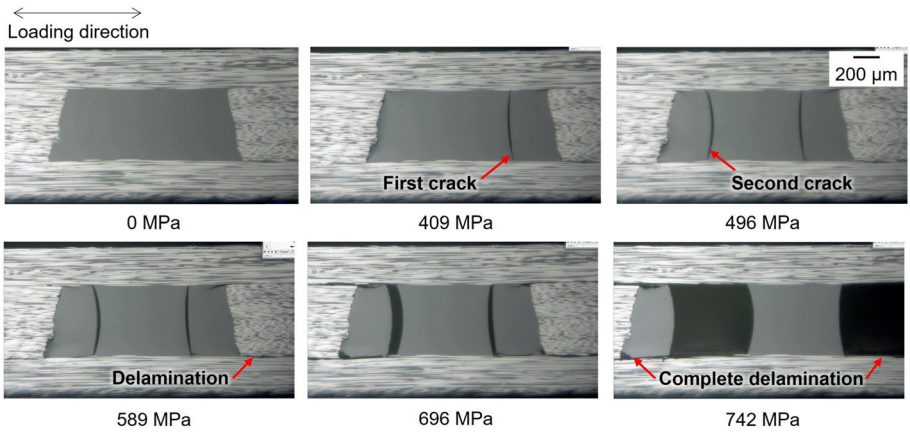


Fig. 5 Microscopic images of laminate edge (specimen 2) with 1.38-mm resin gap at different stress levels

The edge observations of the specimens with resin gap lengths of 1.38 mm (specimen 2), 1.73 mm (specimen 3), and 3.41 mm (specimen 4) are shown in Figs. 5, 6, and 7, respectively. For specimens with a resin gap length of around 1 mm, although the exact crack locations with respect to the interfaces and the stresses varied slightly, the presented cracking pattern is representative of all tested specimens of similar resin pocket geometry and length. For this case, three specimens with resin pocket lengths ranging from 1.25 mm to 1.4 mm were tested. Taking the example of laminate with a 1.38-mm resin gap length, there are several aspects of the observed crack pattern that should be noted in the laminates (see Fig. 5):

(i) A crack in the resin pocket followed insignificant small fiber–matrix debonding at the interface edge of resin and discontinuous CFRP ply(s).
(ii) The first crack forms not at the interface, but at a distance from the interface between the resin and the discontinuous UD ply (at 409 MPa).
(iii) The secondary cracks appear closer to the interface at higher stresses in the fragments bounded by the initial crack and the interface with the discontinuous ply, while the longer fragments develop a crack first (at 496 MPa). In some specimens, a third (left) crack was observed.
(iv) All cracks in the resin region curve toward the center of the region, while successively formed cracks demonstrate higher curvatures (compare the crack patterns at 409 and 496 MPa).
(v) Matrix cracking is followed by delamination cracks growing in opposite directions from the matrix cracks toward the ends of the specimen (around or before 696 MPa). This validated a sudden decrease in the slope of the stress–strain curve in Fig. 3 (b) before the ply discount phenomenon at an applied stress of 742 MPa.
(vi) Strain readings from strain gauge 1 confirmed a linear elastic stress–strain behavior between crack occurrences until the inception of delamination cracks. Clear strain jumps were observed at the applied stresses of crack occurrences, which was validated by optical monitoring (compare Figs. 3 (b) and 5).
(vii) The interface between the resin region and the UD ply does not fail; the bond between the resin material and the discontinuous ply remains preserved, although darkened areas close to the corners of the pocket at higher loads imply local damage development (Fig. 5 at applied stresses of 589 and 696 MPa).

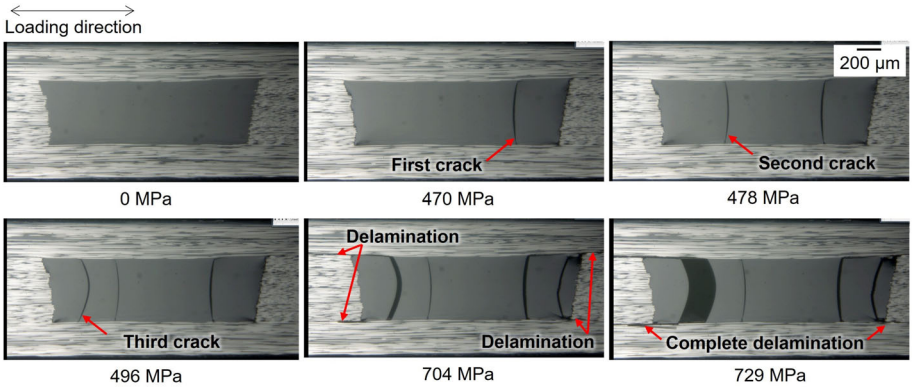


Fig. 6 Microscopic images of laminate edge (specimen 3) with 1.73-mm resin gap at different stress levels

A similar observation for laminate with a resin pocket length of 1.24 mm has been reported and explained in [29]. In order to explain the location of the first crack observed (observation (i)), recall that the resin region underwent curing with the rest of the laminate. Epoxy resin demonstrates significant shrinkage while curing, with more than a 6% volumetric change, e.g., [39, 40]. In the confined conditions of the resin surrounded by UD plies, shrinkage introduces hydrostatic tension and residual stresses at the end of the post-gelation shrinkage stage, similar to what occurs at the micro-scale in a resin-reach zone surrounded by closely packed fibers. The phenomenon seen in observation (iii) is similar to the curved or oblique cracks that have previously been observed in the thick transverse ply of cross-ply laminates [41–44]. The cracks are believed to originate near previously formed plane transverse cracks at the peak of the first (maximum) principal stress along the interface between the axial and transverse plies along the trajectory of the second (minimum) principal stress, which exists in the transverse ply before the crack appears [41].

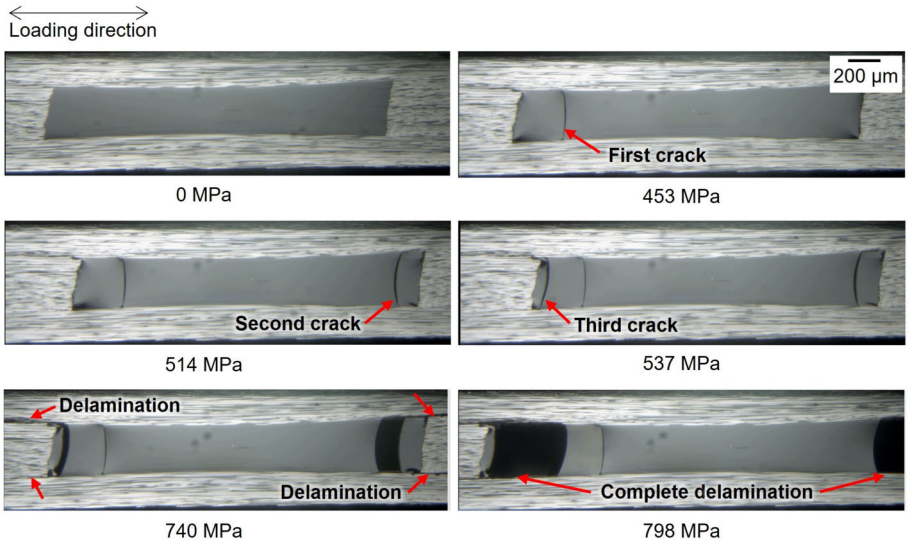


Fig. 7 Microscopic images of laminate edge (specimen 4) with 3.41-mm resin gap at different stress levels

For the laminate with a longer resin gap length of 1.73 mm (Fig. 6), almost the same damage behavior as described above for the laminate with a gap length of 1.38 mm was observed despite having a total of four cracks in the resin pocket. The only difference in the crack pattern that might have caused the change in the number of cracks is that the second crack occurred further from the interface between the resin and UD ply compared to the fragment length bounded by the first crack and the interface. The high axial stress that might exist in the longer fragment bounded by the second crack and the interface on the left side could potentially allow a new crack to form. Comparing this result to the stress–strain curve in Fig. 3 (c), the strain jumps caused by the formation of cracks in the resin pocket also resemble the observed cracks on the edge of the specimen.

The same behavior was expected to occur in the specimens with longer resin gaps, such as the 3.41 mm specimen, Fig. 7 shows that only three cracks occurred in the resin pocket. This result depends on the location of the crack, which is highly sensitive to the geometry of the resin pocket, especially the resin gap length and the uniformity in the width direction of the specimen. In addition, as observed in the laminates with a longer resin gap (e.g., Fig. 7), besides having non-straight resin–UD ply interfaces, the UD fibers located above and below the resin pocket (around the middle) curved towards the middle of the laminate in the thickness direction. This might have occurred during the lamination process of the prepreg composites when the upper and lower continuous plies were attached with some force to the middle plies or have resulted from the curing process as the applied pressure pushed the upper and lower continuous plies into the blank (ply discontinuous) region left for the resin. Consequently, the stress distribution in the resin pocket might behave differently compared to a straight-uniform square-shaped resin pocket, which eventually causes some variations in the damage behavior. This might explain why no third crack occurred in the specimens with a resin gap around 1 mm (Specimens 2, 3) described above, as the geometry of the resin pocket of each specimen might differ. For the laminates with long resin gaps, close to 2 mm and 3 mm, at least two specimens for each case were tested, and similar damage behavior was observed.

Further investigation was conducted using X-ray CT to understand the damage behavior inside the resin pocket and confirm that the cracks occurred not at the interface but at a distance from the interface between the resin and the discontinuous UD ply. A UD laminate with a resin gap length of 1.48 mm was used. To understand the damage mechanism as the load increased, the specimen was loaded and unloaded three times, with X-ray CT scans performed after each unloading. The first and second loadings were performed until the first and second cracks, respectively, were observed on the edge of the specimen. The final loading was conducted until some delamination from the tips of matrix cracks was visible on the edge, i.e., before complete delamination occurred between the continuous and discontinuous plies. The final scan results are shown in Fig. 8. The x-axis is the loading direction, the y-axis is the width, and the z-axis is the thickness of the specimen. The image on the left shows the edge view observation, while the right image shows the cross-sectional view in the z-direction (x-y plane). By examining the location of Crack 1, it can be seen that the crack did not propagate along the interface between the resin and the discontinuous UD ply but rather propagated away from the interface, although, at one point, it did touch the interface. This was also observed for Cracks 2 and 3 after the second loading.

From the edge observation results for a specimen with a similar resin gap length in Fig. 5, only two cracks were initially observed on the edges. However, the X-ray CT scan revealed that the second crack did not propagate fully along the width direction, and an additional crack (Crack 3) occurred at approximately the same location on the opposite edge. Both of these cracks occurred at roughly the same applied load. This explains the strain jump

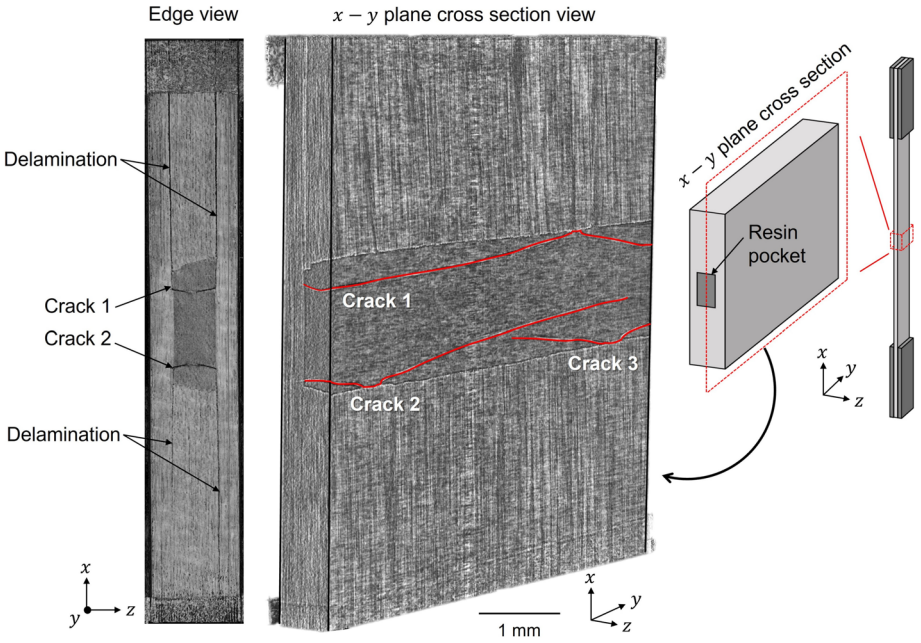


Fig. 8 X-ray CT results showing damage in and around the resin pocket of a laminate with a 1.48-mm gap

observed in the stress–strain curve of a different specimen with a similar resin gap length (labeled as X in Fig. 9), even though only two cracks ((a) and (b)) were visible on the edge of the specimen. This behavior might result from the drastic change in stress distribution within the resin pocket after the first crack formation. The redistribution of stresses caused by a

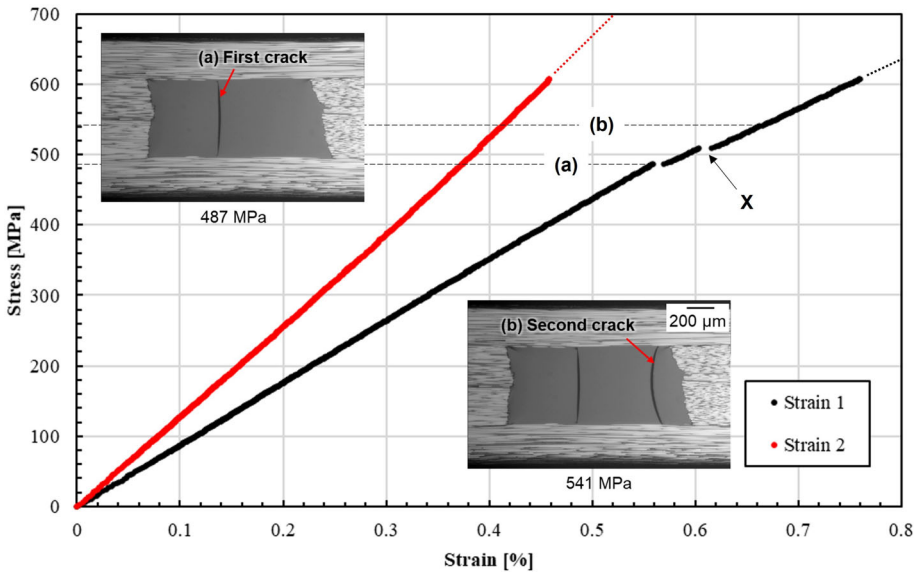


Fig. 9 Stress–strain curve and optical observations showing the presence of first and second cracks in laminate with 1.26-mm resin gap

drop in axial stresses and a perturbation in shear stress may have slowed the propagation of the second and third cracks from the edges, and as a result, they did not meet in the middle. Similar to Crack 1, both Crack 2 and Crack 3 formed in a V-shape in the width direction. They touched the UD ply–resin interface once but predominantly moved away from it.

4 Analytical Prediction of the Crack Initiation using A Variational Approach

An analysis introduced by the authors in a previous study [35] was used in this work to predict crack initiation in the resin pocket for different resin pocket lengths. This stress-based variational analysis for composite laminates with ply discontinuities is based on an approach introduced by Hashin in 1985 [45]. Figure 10 shows the analysis model used in this study. The simplified geometry consists of a rectangular resin region with a thickness t_1, length L_0, and unit depth. The interfaces between the resin pocket and the discontinuous ply, as well as the cracks within the resin, are assumed to be flat and perpendicular to both the laminate surface and the loading direction (x). This assumption is considered valid for cracks with minimal curvature. An admissible stress field was constructed for a laminate containing a resin pocket, with or without cracks, which satisfies the conditions of equilibrium within the laminate, traction continuity at the interfaces between the resin pocket and the discontinuous UD ply, zero traction on external and open crack surfaces, and minimization of the complementary energy functional.

The analytical derivation procedure used in this paper is essentially the same as that introduced in [35]. In this analysis, the boundary stresses of the resin pocket region that minimize the complementary energy were determined to solve the stress functions. To predict cracking, the finite fracture criterion was employed to describe the onset of matrix cracks in the resin pocket. For laminates developing a through-the-ply crack at a specific location, x, the critical ERR, G_C, was calculated as:

$$G_C = \frac{\Delta U_{\text{ca}}(x)}{\Delta A_c}, \tag{1}$$

where $\Delta U_{\text{ca}}(x)$ is the change in complementary energy due to crack occurrence at x, and ΔA_c is the crack area. In the present case, the ERR associated with crack formation was defined as:

$$G_C = \frac{(U'_{\text{ca}} - U_{\text{ca}})\,\sigma_C^2}{A_c\,\sigma_0^2}, \tag{2}$$

where U'_{ca} and U_{ca} are the complementary energies of the cracked and uncracked laminates, respectively, σ_C is the crack onset stress obtained from experimental results, and σ_0 is the applied axial stress. The crack onset stresses for laminates with varying resin pocket lengths

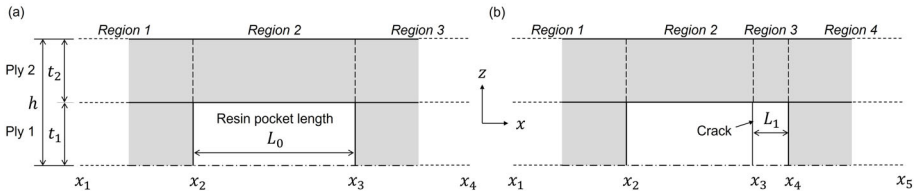


Fig. 10 Variational analysis model. (a) Uncracked model, (b) Cracked model

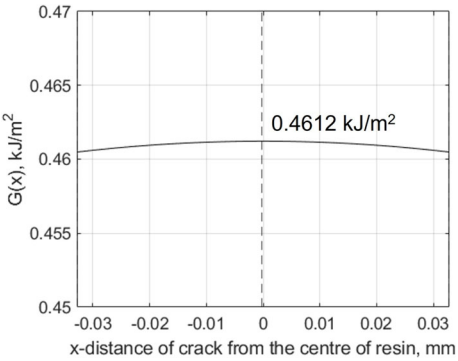


Fig. 11 ERR as a function of the x-distance of the crack from the center of the resin pocket for a laminate with four discontinuous plies and a resin pocket length of 0.0656 mm

were calculated using:

$$\sigma_C = \sqrt{\frac{A\,\sigma_0^2\,G_C}{U'_{\text{ca}} - U_{\text{ca}}}}. \tag{3}$$

Here, the material properties of the CFRP ply measured in [36] were used. The properties of the epoxy resin were assumed to be $E = 3$ GPa and $\nu = 0.3$.

Figures 11 and 12 show the ERR as a function of the x-distance of the crack from the center of the resin pocket for a laminate with resin pocket lengths of 65.6 μm and 1.73 mm, respectively. These two laminates are presented as representatives of a laminate with a very short resin pocket length (< 0.1 mm) and a laminate with a long resin pocket length. The calculated maximum ERR associated with the crack location determines the critical ERR (G_c). For the specimen with a very short resin pocket, G_c was estimated to be 461.2 J/m^2, while for the specimen with a long resin pocket, G_c was estimated to be 570.3 J/m^2. For the laminate with a very short resin pocket, the ERR reaches its maximum at the center of the resin pocket (Fig. 11); however, the ERR values do not vary significantly across different x-distances. Experimentally, it is also challenging to define the exact location of the crack when the resin pocket is very short (Fig. 4). On the other hand, for the laminate with a long resin pocket, the ERR reaches its maximum at the interface between the CFRP ply and the resin pocket (Fig. 12). However, this observation does not explain the cracking pattern observed in Fig. 6, which is related to the effects of chemical shrinkage of the resin as explained above. This discrepancy arises because the analysis in this study did not account for these effects.

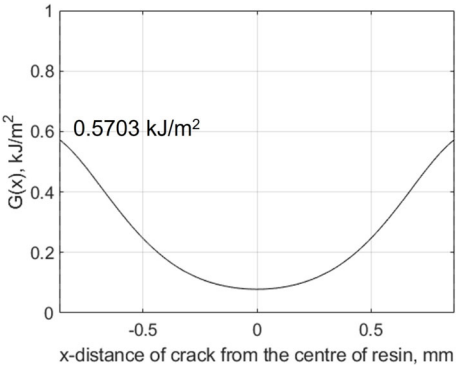


Fig. 12 ERR as a function of the x-distance of the crack from the center of the resin pocket for a laminate with four discontinuous plies and a resin pocket length of 1.73 mm

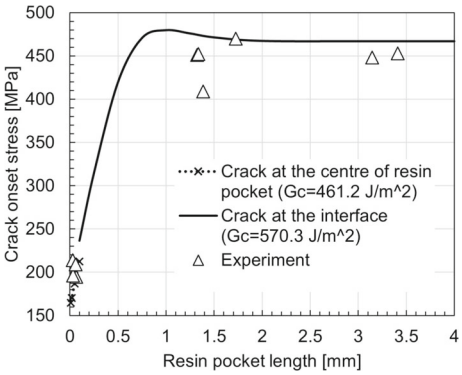


Fig. 13 Prediction of crack onset stress for laminates with different resin pocket lengths, compared to experimental results. The predictions assume that the crack occurs at (a) the center of the specimen ($G_c = 461.2$ J/m^2) or (b) the interface between the CFRP ply and the resin pocket ($G_c = 570.3$ J/m^2)

Based on the results in Figs. 11 and 12, the location of the crack was assumed differently for the prediction of crack onset stresses in laminates with varying resin pocket lengths. For laminates with a resin pocket length of less than 0.1 mm, the crack was assumed to initiate at the center of the resin pocket. Conversely, for laminates with a resin pocket length exceeding 0.1 mm, the crack was assumed to initiate at the interface between the UD ply and the resin pocket, based on the maximum energy release rate criterion applied in this study. Figure 13 shows the prediction of crack onset stress for laminates with different resin pocket lengths, compared to experimental results. Figure 14, on the other hand, provides an enlarged view of Fig. 13 for resin pocket lengths less than 0.1 mm. The results demonstrate that the analytical predictions are in good agreement with the experimental results.

The stress-based variational analysis used in this study, which employs the minimum complementary energy based on Hashin's variational model [45], has demonstrated its capability to calculate the energy release rate and predict crack onset stresses in laminates with ply discontinuities. However, it should be noted that this analysis utilizes a plane stress approach for simplicity, which restricts its application to simple material configurations such as UD and cross-ply laminates. To broaden the applicability of the analysis, it is necessary to account for stress components in the width direction of the laminate. Additionally, thermal effects, including the consideration of chemical shrinkage in the resin pocket, which were not included in the current analysis, should be incorporated into future studies to enhance the accuracy of cracking predictions. Moreover, adopting natural boundary conditions, as

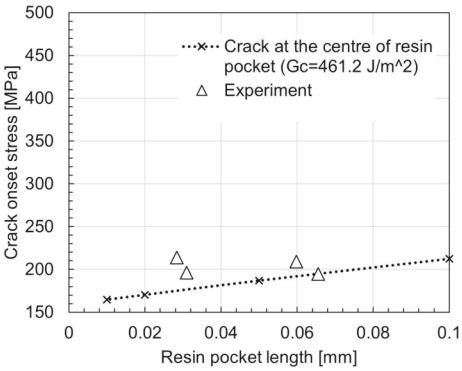


Fig. 14 Enlarged view of the prediction of crack onset stress for laminates with different resin pocket lengths, shown in Fig. 8, for laminates with resin pocket lengths less than 0.1 mm

implemented in [46, 47], and/or a ply refinement technique [48, 49], could help overcome the limitations of the two-ply system and further improve the accuracy of the analysis.

This study has primarily focused on the damage behavior within the resin pocket without performing a detailed examination of delamination initiation and propagation. While the findings offer valuable insights into matrix cracking and stress distribution within the resin pocket, delamination plays a critical role in the overall structural integrity of CFRP laminates. Further investigation into the delamination mechanisms, particularly initiation and propagation from the tips of matrix cracks, is essential. These findings will be explored and published in a subsequent paper, building on the groundwork laid in the current study. Additionally, the insights gained from this experimental characterization provide an opportunity to explore the mechanical properties, damage behavior, and failure mechanisms in more complex laminate configurations, such as angle-ply, quasi-isotropic laminates, and tapered laminate structures, which are closer to real-world applications. The findings can also be a foundation for developing predictive models and simulations. Future research should prioritize the development of accurate, validated computational models to simulate the unintuitive cracking behavior observed in this study and predict damage evolution in CFRP laminates with ply discontinuities. These models would be valuable tools for optimizing laminate design and improving damage tolerance, ultimately enhancing the performance of composite structures in various applications.

5 Conclusions

This study conducted a detailed investigation into the material properties and damage behavior of UD laminates with ply discontinuities, focusing on varying resin gap lengths. Key findings from the results include:

(i) Cracks form not at the interface between the resin and the discontinuous UD ply but at a distance from the interface, likely due to the significant shrinkage of epoxy resin during the curing process.
(ii) Secondary cracks appear closer to the interface at higher stress levels in the fragments bounded by the initial crack and the interface, with longer fragments developing cracks first.
(iii) Cracks in the resin region tend to curve toward the center, with successively formed cracks exhibiting higher curvature due to the redistribution of principal stresses within the resin pocket after the initial crack(s).
(iv) Matrix cracking is followed by delamination cracks that propagate from the matrix cracks toward the ends of the specimen.
(v) X-ray CT observations provide valuable insights into the internal damage within the resin pocket, revealing multiple cracks that were not visible on the edges of the specimen.

In addition to the experimental investigation, a stress-based variational analysis was employed to predict crack onset stresses in laminates with ply discontinuities. The analysis successfully calculated the ERR for laminates with varying resin pocket lengths and provided predictions for crack onset stresses. The analytical predictions showed good agreement with the experimental observations, enhancing the understanding of resin pocket behavior in CFRP laminates.

This study used constant-thickness laminate with a resin pocket to isolate the effects of ply discontinuity on damage propagation specifically, without the additional complexity introduced by thickness variation. This controlled setup allows a clearer interpretation of how

resin pockets impact matrix cracking. The findings from this study can be used as a benchmark for understanding resin pocket behavior in tapered laminates. Future work will address the exploration of delamination mechanisms and investigate other laminate configurations or more complex structures to further enhance the understanding of damage behavior in CFRP laminates.

Author Contributions M.F. conducted the experiments, collected data and analysis. Y.A. and R.I. assisted in conducting the experiments and contributed to data collection. V.V. performed data analysis and developed the theoretical framework. K.T. and S.O. conceptualized the study and supervised the research. M.F. and V.V. wrote the main manuscript text. All authors reviewed and approved the final manuscript.

Funding A part of this work was supported by JKA and its promotion funds from KEIRIN RACE received by one of the co-authors (S. Ogihara).

Data Availability No datasets were generated or analysed during the current study.

Declarations

Competing interests The authors declare no competing interests.

Ethics approval and consent to participate: Not applicable

Open Access This article is licensed under a Creative Commons Attribution 4.0 International License, which permits use, sharing, adaptation, distribution and reproduction in any medium or format, as long as you give appropriate credit to the original author(s) and the source, provide a link to the Creative Commons licence, and indicate if changes were made. The images or other third party material in this article are included in the article's Creative Commons licence, unless indicated otherwise in a credit line to the material. If material is not included in the article's Creative Commons licence and your intended use is not permitted by statutory regulation or exceeds the permitted use, you will need to obtain permission directly from the copyright holder. To view a copy of this licence, visit http://creativecommons.org/licenses/by/4.0/.

References

1. Ogihara, S., Takeda, N.: Interaction between transverse cracks and delamination during damage progress in CFRP cross-ply laminates. Compos. Sci. Technol. **54**(4), 395–404 (1995)
2. Yokozeki, T., Aoki, Y., Ogasawara, T.: Experimental characterization of strength and damage resistance properties of thin-ply carbon fiber/toughened epoxy laminates. Compos. Struct. **82**(3), 382–389 (2008)
3. Deng, H., Mochizuki, A. Fikry, M.J., Abe, S., Ogihara, S., Koyanagi, J.: Numerical and experimental studies for fatigue damage accumulation of CFRP cross-ply laminates based on entropy failure criterion. Materials **16**(1) (2023)
4. Ogihara, S., Takeda, N., Kobayashi, S., Kobayashi, A.: Effects of stacking sequence on microscopic fatigue damage development in quasi-isotropic CFRP laminates with interlaminar-toughened layers. Compos. Sci. Technol. **59**(9), 1387–1398 (1999)
5. Ramesh, T., Singh, C.V.: Damage and failure of composite materials. Cambridge University Press, Cambridge New York (2012)978-0-521-81942-8
6. Mack, J.P., Mirza, F., Banik, A., Khan, M.H., Tan, K.T.: Hybridization of face sheet in sandwich composites to mitigate low temperature and low velocity impact damage. Compos. Struct. **338**, 118101 (2024)
7. Koyanagi, J., Mochizuki, A., Higuchi, R., Tan, V.B.C., Tay, T.E.: Finite element model for simulating entropy-based strength-degradation of carbon-fiber-reinforced plastics subjected to cyclic loadings. Int. J. Fatigue **165**, 107204 (2022)
8. Isaac, C.W., Ezekwem, C.: A review of the crashworthiness performance of energy absorbing composite structure within the context of materials, manufacturing and maintenance for sustainability. Compos. Struct. **257**, 113081 (2021)

9. Willmann, E., Boll, B., Scheel, M., Meißner, R.H., Fiedler, B.: Health monitoring of CFRP laminates under cyclic loading via vibro-acoustic modulation based measurements. Compos. Struct. **308**, 116696 (2023)
10. Varughese, B., Mukherjee, A.: A ply drop-off element for analysis of tapered laminated composites. Compos. Struct. **39**(1), 123–144 (1997)
11. Abdulhamid, H., Bouvet, C., Michel, L., Aboissière, J., Minot, C.: Influence of internally dropped-off plies on the impact damage of asymmetrically tapered laminated CFRP. Compos. Part A: Appl. Sci. Manufact. **68**, 110–120 (2015)
12. Mirza, F., Mack, J.P., Banik, A., Khan, M.H., Tan, K.T.: Post impact flexural behavior investigation of hybrid foam-core sandwich composites at extreme arctic temperature. Compos. Sci. Technol. **258**, 110897 (2024)
13. Ahamed, J., Joosten, M., Callus, P., Wisnom, M.R., Wang, C.H.: Ply-overlap hybrid technique for joining dissimilar composite materials. Mater. Des. **100**, 157–167 (2016)
14. Xie, C., Wan, Y., Wang, L., Yu, X., Ma, Y.: Experimental investigation on the compression-after-double-impact behaviors of GFRP laminates embedded with aluminum mesh. Polym. Compos. 1–11 (2024)
15. Ravichandran, B., Balasubramanian, M.: Joining methods for fiber reinforced polymer FRP composites a critical review. Compos. Part A: Applied Science and Manuf. **186**, 108394 (2024)
16. Chen, Y., Wan, Y., Li, C., Zhang, J.: Tensile behavior of mechanical joint for GFRP/metal mesh hybrid laminate after low-velocity impact. Polym. Compos. 1–14 (2025)
17. Endalew, A.M., Woo, K., Cairns, D.S.: Effect of drilling-induced defects on progressive damage of open-hole composite laminates under compression. Adv. Compos. Mater. **31**(4), 399–427 (2022)
18. Zhang, Y., Zhou, Z., Pan, S., Tan, Z.: Comparison on failure behavior of three-dimensional woven carbon/carbon composites joints subjected to out-of-plane loading at room and high temperature. Compos. Commun. **23**, 100567 (2021)
19. Oromiehie, E., Prusty, B.G., Compston, P., Rajan, G.: Automated fibre placement based composite structures: Review on the defects, impacts and inspections techniques. Compos. Struct. **224**, 110987 (2019)
20. Minakuchi, S., Simacek, P., Advani, S.G.: In-situ consolidation deformation of composite laminate with gaps of various widths. Compos. Part A: Appl. Sci. Manuf. **180**, 108054 (2024)
21. Cui, W., Wisnom, M.R., Jones, M.: An experimental and analytical study of delamination of unidirectional specimens with cut central plies. J. Reinf. Plast. Compos. **13**(8), 722–739 (1994)
22. Ganesan, R., Liu, D.Y.: Progressive failure and post-buckling response of tapered composite plates under uni-axial compression. Compos. Struct. **82**(2), 159–176 (2008)
23. Fikry, M.J., Vinogradov, V., Ogihara, S.: Mechanical properties and damage behavior of tapered unidirectional CFRP laminates. Mech. Eng. J. **10**(4), 23–00079–23–00079 (2023)
24. Gan, K.W., Allegri, G., Hallett, S.R.: A simplified layered beam approach for predicting ply drop delamination in thick composite laminates. Mater. Des. **108**, 570–580 (2016)
25. Fish, J., Lee, S.: Delamination of tapered composite structures. Eng. Fracture Mech. **34**, 43–54 (1989)
26. Botting, A.D., Vizzini, A.J., Lee, S.W.: Effect of ply-drop configuration on delamination strength of tapered composite structures. AIAA J. **34**, 1650–1656 (1996)
27. He, K., Hoa, S.V., Ganesan, R.: The study of tapered laminated composite structures: a review. Composit. Sci. Technol. **60**(14), 2643–2657 (2000)
28. Zhang, B., Kawashita, L.F., Jones, M.I., Lander, J.K., Hallett, S.R.: An experimental and numerical investigation into damage mechanisms in tapered laminates under tensile loading. Compos. Part A: Appl. Sci. Manuf. **133**, 105862 (2020)
29. Fikry, M.J., Vinogradov, V., Ogihara, S.: Experimental observation and modeling of resin pocket cracking in unidirectional laminates with ply discontinuity. Compos. Sci. Technol. **218**, 109175 (2022)
30. Nakatani, H., Nakaya, K., Matsuba, A., Kouno, Y., Ogihara, S.: Effect of prepreg cut on the mechanical properties in CFRP laminates. J. Solid Mech. Mater. Eng. **5**(12), 742–752 (2011)
31. Nakatani, H., Nakaya, K., Matsuba, A., Kouno, Y., Ogihara, S.: Damage behavior in unidirectional CFRP laminates with fiber discontinuity. Trans. JSME, Series A **79**(799), 294–303 (2013)
32. Nakatani, H., Nagata, Y., Kitamura, R., Matsuba, A., Kouno, Y., Ogihara, S.: Damage behavior in CFRP laminates containing fiber discontinuities of different sizes. Trans. JSME **81**(831), 15–00226 (2015)
33. Nagata, Y., Nakatani, H., Matsuba, A., Kouno, Y., Ogihara, S.: Effect of fiber discontinuity on mechanical properties of interlaminar-toughened CFRP laminates. Trans. JSME **81**(825), 14–00699 (2015)
34. Fikry, M.J., Wang, Q., Irita, M., Ri, S., Toyama, N., Vinogradov, V., Ogihara, S.: Measurement of microscopic strain distributions of CFRP laminates with fiber discontinuities by sampling moiré method. Adv. Compos. Mater. **31**(3), 273–288 (2022)
35. Fikry, M.J., Vinogradov, V., Ogihara, S.: Analytical prediction of the local young's modulus in CFRP laminate with ply discontinuity: a variational approach. Adv. Compos. Mater. **32**(6), 843–865 (2023)

36. Fikry, M.J., Ogihara, S., Vinogradov, V.: The effect of matrix cracking on mechanical properties in frp laminates. Mech. Adv. Mater. Modern Process. **4**(3), 1–16 (2018)
37. Fikry, M.J., Ogihara, S.: Damage behaviors in cross-ply cloth CFRP laminates cured at different temperatures. Mech. Eng. J. **7**(5), 20–00383 (2020)
38. Fikry, M.J., Terashi, N., Koizumi, K., Ogihara, S.: Inhibition of interlaminar damage in CFRP laminates by inserting non-woven carbon fiber interlaminar reinforced tissue. Adv. Compos. Mater. 1–21 (2024)
39. Zarrelli, M., Skordos, A.A., Partridge, I.K.: Investigation of cure induced shrinkage in unreinforced epoxy resin. Plast. Rubber Compos. **31**(9), 377–384 (2002)
40. Kravchenko, O.G., Li, C., Strachan, A., Kravchenko, S.G., Pipes, R.B.: Prediction of the chemical and thermal shrinkage in a thermoset polymer. Compos. Part A: Appl. Sci. Manuf. **66**, 35–43 (2014)
41. Groves, S.E., Harris, C.E., Highsmith, A.L., Allen, D.H., Norvell, R.G.: An experimental and analytical treatment of matrix cracking in cross-ply laminates. Exper. Mech. **27**(1), 73–79 (1987)
42. Hu, S., Bark, J.S., Nairn, J.A.: On the phenomenon of curved microcracks in [(s)/90n]s laminates: Their shapes, initiation angles and locations. Compos. Sci. Technol. **47**(4), 321–329 (1993)
43. Jalalvand, M., Wisnom, M.R., Hosseini-Toudeshky, H., Mohammadi, B.: Experimental and numerical study of oblique transverse cracking in cross-ply laminates under tension. Compos. Part A: Appl. Sci. Manuf. **67**, 140–148 (2014)
44. Fikry, M.J., Ogihara, S., Vinogradov, V.: Application of dic to deformation measurement around damages in CFRP cross-ply laminates. Mech. Eng. J. **6**(3), 19–00003 (2019)
45. Hashin, Z.: Analysis of cracked laminates: a variational approach. Mech. Mater. **4**(2), 121–136 (1985)
46. Hajikazemi, M., Sadr, M.H.: A variational model for stress analysis in cracked laminates with arbitrary symmetric lay-up under general in-plane loading. Int. J. Solids Struct. **51**(2), 516–529 (2014)
47. Hajikazemi, M., Sadr, M.H.: Stiffness reduction of cracked general symmetric laminates using a variational approach. Int. J. Solids Struct. **51**(7), 1483–1493 (2014)
48. Hajikazemi, M., Sadr, M.H., Hosseini-Toudeshky, H., Mohammadi, B.: Thermo-elastic constants of cracked symmetric laminates: A refined variational approach. Int. J. Mech. Sci. **89**, 47–57 (2014)
49. Vinogradov, V.: A variational method for analysis of laminates with parallel arrays of intralaminar cracks. Int. J. Numerical Methods Eng. **120**(5), 666–705 (2019)

Publisher's Note Springer Nature remains neutral with regard to jurisdictional claims in published maps and institutional affiliations.

Authors and Affiliations

M. J. Mohammad Fikry[1,2] · Yutaro Arai[3] · Ryo Inoue[4] · Vladimir Vinogradov[5] · K. T. Tan[2] · Shinji Ogihara[1]

✉ M. J. Mohammad Fikry
fikry@rs.tus.ac.jp

Yutaro Arai
arai.yutaro@rs.tus.ac.jp

Ryo Inoue
inoue.ryo@rs.tus.ac.jp

Vladimir Vinogradov
vladimir.vinogradov@ncl.ac.uk

K. T. Tan
ktan@uakron.edu

Shinji Ogihara
ogihara@rs.tus.ac.jp

[1] Department of Mechanical and Aerospace Engineering, Tokyo University of Science, 2641, Yamazaki, Noda-shi 278-8510, Chiba-ken, Japan

[2] Department of Mechanical Engineering, University of Akron, 244 Sumner St, Akron 44325-3903, Ohio, United States

[3] Department of Materials Science and Technology, Tokyo University of Science, 6-3-1, Niijuku, Katsushika-ku 125-8585, Tokyo, Japan

[4] Department of Mechanical Engineering, Tokyo University of Science, 6-3-1, Niijuku, Katsushika-ku 125-8585, Tokyo, Japan

[5] School of Engineering, Newcastle University, Drummond Building, Newcastle upon Tyne NE1 7RU, Newcastle upon Tyne, United Kingdom